Chinese Chemical Letters 31 (2020) 654–666

Contents lists available at ScienceDirect

Chinese Chemical Letters

journal homepage: www.elsevier.com/locate/cclet

Review

SiO_x-based ($0 < x \leq 2$) composites for lithium-ion batteries

Tong Wang[a,1], Xiaotian Guo[b,1], Huiyu Duan[a], Changyun Chen[a,*], Huan Pang[b]

[a] College of Environmental Science, Nanjing Xiaozhuang University, Nanjing 211171, China
[b] School of Chemistry and Chemical Engineering, Guangling College, Yangzhou University, Yangzhou 225009, China

ARTICLE INFO

Article history:
Received 18 May 2019
Received in revised form 20 May 2019
Accepted 20 May 2019
Available online 8 June 2019

Keywords:
Lithium-ion battery
Anode material
SiO_2 composites
SiO composites
SiO_x-based ($0 < x \leq 2$) composite

ABSTRACT

Silicon (Si) materials as anode materials for applications in lithium-ion batteries (LIBs) have received increasing attention. Among the Si materials, the electrochemical properties of SiO_x-based ($0 < x \leq 2$) composites are the most prominent. However, due to the cycling stability of SiO_x being far from practical, there are some problems, such as low initial coulombic efficiency (ICE), obvious volume expansion and poor conductivity. Researchers in various countries have optimized the electrochemical properties of SiO_x-based composites by means of pore formation, surface modification, and the choice of constituents. In this review, SiO_x-based composites are classified into three categories based on the valency of Si (SiO_2 composites, SiO composites and SiO_x ($0 < x < 2$) composites). The synthesis, morphologies and electrochemical properties of the SiO_x-based composites that are applied in LIB are discussed. Finally, the properties of several common SiO_x-based composites are briefly compared and the challenges faced by SiO_x-based composites are highlight.

1. Introduction

In order to achieve sustainable development, electric energy replaces fossil energy, greatly reducing energy and environmental pressures. Therefore, energy storage equipment has become a hot topic in the world. Lithium ion battery (LIB) is one of the most attractive devices in energy storage equipments. In 1991, Sony [1] let LIBs enter the eyes of people for the first time and apply them to people's lives. LIBs have become more and more widely used due to their unique advantages such as light weight, compact structure, high energy density and long cycle life [2–4]. LIBs are not only widely applied in devices such as watches, laptops, electric vehicles and medical equipment but are also considered as potential candidates for fossil fuel substitutes [5–7]. They can provide clean energy to vehicles and alleviate the environmental hazards of fossil fuels.

Anode materials are an important part of LIBs, and they are closely related to the energy density, cycling life and safety performance of the batteries. Thus, finding a suitable electrode material is the key to enhancing the electrochemical performance of LIBs. Common LIB anode materials include carbon materials, Si-related materials and metal-oxide materials. Carbon material is the earliest anode material of LIB [8–12]. As early as 1996, Shi *et al.* [13] studied the structure and lithium intercalation properties of graphite. Later, some studies found that graphite electrodes as anode material of LIBs have low energy density (375 mAh/g) and safety issues [14,15]. Due to these problems, the market development of graphite electrodes has been limited. Metal oxides (MO_x) [16–19] and Si-related composites [20–26] are regarded as potential anode materials for next-generation LIBs. Although Si has an extremely high theoretical capacity (4200 mAh/g), the use of Si-based anodes is limited by the excessive volume change (up to 400%) of Si during a single cycle. Therefore, it is necessary to modify Si with the aim of improving the electrochemical performance of Si-based negative electrodes. The main improvement methods generally involve surface treatment, multiphase doping, and silicide formation. Uday [27], Wei [28] and Ma *et al.* [29] synthesized C-Si composites, porous interlayer G/Si nanocomposites (PG-Si) and yolk-shell structured Si-C nanocomposites, respectively, to slow the volume expansion of Si. In the process of improving these Si-based materials, researchers found that SiO_x-based materials have better electrochemical performance and commercial prospects. Compared to Si-based materials, the use of SiO_x-based materials can decrease the initial irreversible capacity, slow the expansion of bulk, and improve the cycle performance [30–34]. Additionally, the cost of preparing SiO_x-based materials is relatively lower than that for Si materials. It was found that LIBs based on SiO_x materials showed increased cycling stability and a decreased specific capacity with an increasing the value of x in SiO_x [35,36]. To this end, in recent years, many researchers began to

* Corresponding author.
E-mail address: cychen@njxzc.edu.cn (C. Chen).
[1] These authors contributed equally to this work.

https://doi.org/10.1016/j.cclet.2019.06.002

study SiO_x composite materials as LIB anode materials. To improve the cycling stability of SiO_x, Dirican [24], Kim [37] and Zhang *et al.* [38] synthesized SiO_2-confined Si/C nanofiber composites, SiO-C composites and nano-Si@SiO_x@C composites, respectively. To increase the cycling life of LIBs based on SiO_x, Kurc [39] and Dai *et al.* [40] prepared $Li_4Ti_5O_{12}/SiO_2$ composites and amorphous Si/SiO_x/SiO_2 nanocomposites, respectively. To improve the conductivity and reversible capacity and reduce the volume expansion of SiO_x, Cui [41], Woo [42] and Bae *et al.* [43] manufactured microsized porous C/SiO_2 composites, boron-doped SiO composites and TiO_{2-x}@Si/SiO_x nanospheres, respectively. It can be seen from these improved composite materials that SiO_x-based materials are developing in the direction of porous structure and multiphase recombination.

In terms of employing Si-related materials as anode materials for LIBs, a few of the earlier reviews summarized the application of Si-based materials and SiO_x materials. Zhu *et al.* [44] compared and discussed various methods for preparing Si and Si-based anodes and explored the future development of Si-based composites. Luo *et al.* [45] summarized the technical issues and feasible solutions of nano-Si/C composite anodes for LIBs. Li *et al.* [46] briefly studied the mechanism of Li-Si alloying and battery failure, summarized and solved the known problems of nanostructured Si materials, nano/microstructured Si/C and SiO_x/C anodes, and finally proposed a forward-looking outlook for Si-based materials in practical applications. Chen *et al.* [47] reviewed the electrochemical properties of SiO_x and its related mechanisms, and briefly discussed and proposed research angles and tactics for further improvement of SiO_x properties. However, to our knowledge, SiO_x-based composites as negative LIB electrodes have not been reported.

This review focuses on the synthesis and application of SiO_x-based composites, including SiO_2 composites, SiO composites and SiO_x $(0<x<2)$ composites (Fig. 1), for LIB electrodes. In each section, the electrochemical properties and existing problems of SiO_x-based composites as LIB anode materials are discussed. However, the situation of SiO_x-based composite materials in practical applications is not summarized. Notably, the possible factors affecting the electrochemical properties of SiO_x-based composites and the future development of SiO_x-based composite anode materials are summarized. It is anticipated that SiO_x-based composites will become promising anode materials for LIBs, and we hope that this summary of pioneering research will be of great value and encourage the further development of SiO_x-based composites for LIB applications.

2. SiO_2 composites

SiO_2 composites are the most commonly used materials in SiO_x-based composites given that SiO_2 is inexpensive, easy to synthesize, and commercially viable. Various attempts have been made towards the synthesis of SiO_2 composites. Due to differences in materials and properties and the means of compositing, the resultant properties of composites also differ (as shown in Table 1).

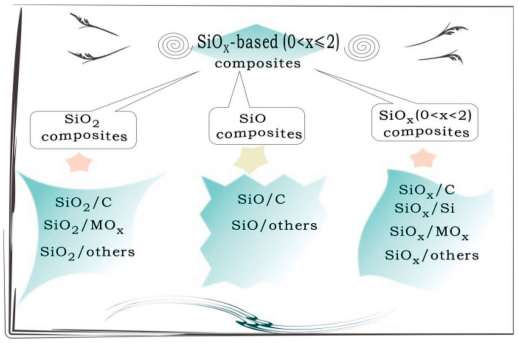

Fig. 1. Conspectus of three major type composites: SiO_2 composites, SiO composites and SiO_x $(0<x<2)$ composites.

2.1. SiO_2/C composites

Carbon has some excellent electrochemical properties: (1) high electrical conductivity [48] (it can promote the electrochemical reaction of materials); (2) relatively good ductility [27]; (3) not large volume change during inserting and deintercalating lithium [49]; and (4) good compatibility with conventional electrolytes [49]. One important strategy for improving the electrochemical performance of SiO_2-based anodes is to coat SiO_2 with conducting shells comprising carbon or carbon-based materials to form SiO_2/C composites.

According to the different carbon sources and different nanostructures used for the composites, the synthesis methods used by researchers mainly include the hydrothermal method [50–52], self-assembly [53], mechanical grinding [54] and chemical vapor deposition (CVD) [55]. Li *et al.* designed and fabricated mesoporous SiO_2 nanospheres (MSNs) and flake graphite (FG) nanocomposites (pp-MSNs/FG) with a shape similar to plum-pudding by a simple, inexpensive hydrothermal method. Firstly, the MSNs, citric acid (binder) and flake graphite were mixed in distilled water, and then performed by hydrothermal treatment and calcination under a nitrogen atmosphere. Fig. 2e briefly depicts the pp-MSNs/FG nanocomposite' preparation procedure. The morphologies of the MSNs and the pp-MSNs/FG nanocomposites were visualized by SEM and TEM. The MSNs were spherical with a diameter of ~ 130 nm (Figs. 2a and b) and well anchored to the FG, forming a structure similar to plum pudding (Figs. 2c and d). As a result of this distinct plum-pudding architecture, the pp-MSNs/FG nanocomposites electrodes exhibited a reversible capacity of 702 mAh/g after 100 cycles at 100 mA/g and excellent rate performance. Xia *et al.* [51] also prepared porous SiO_2/C composites with the hydrothermal method and proved that the electrochemical performance of the SiO_2/C composites improved in terms of Li storage due to its uniquely porous structure. Later, Liang *et al.* [56] successfully prepared a novel type of *N*-adulterated ordered mesoporous C/SiO_2 (N-OMC/SiO_2) nanocomposites using a multicomponent copolymerization strategy. The high effectiveness of the as-constructed SiO_2/C interface architecture was demonstrated by the high capacity, superior cycling and good rate performance of the N-OMC/SiO_2 electrodes in the Li^+ interposition/extraction reaction procedure.

The use of molecular self-assembly technology to prepare nanomaterials is an emerging technology that has only developed in recent years. Due to the unique interface molecular recognition function of this technology, it has great advantages in the preparation of nanomaterials. Self-assembly is a new method of constructing functional materials at the molecular level. The synthesized products have the advantages of controllable particle size, good dispersibility and outstanding stability. As early as 2014, Wang *et al.* [57] synthesized a GR-enfolded SiO_2 nanotube network (SiO_2-NT/G network) composite by self-assembly of ZnO nanorod templates. At the time, the SiO_2-NT/G network composite was being used as a negative electrode for Li^+ batteries and offered a good lithium-memory capability with a good capacity, cycling lifetime and rate performance, among other aspects. Fig. 3b schematically illustrates the synthetic route used for the SiO_2-NT/G network. Later, Qiang *et al.* [53] fabricated bimodal porous C-SiO_2 (BP-CS) nanocomposites with phenolic resins, tetraethyl orthosilicate and pluronic F127 by applying an extensible volume-to-volume subassembly method. Fig. 3a simply explains the procedure for making the BP-CS nanocomposites. The association of high

Table 1
Electrochemical performance of SiO_2 composites in half-cell testing.

Anode material	References	CD[a]/Cycles/Cycle stability capacity	ICE[b]	Capacity retention
pp-MSNs/FG	[50]	100 mA/g /100/702 mAh/g	40%-45%	
SiO_2/C	[51]	100 mA/g /100/888 mAh/g	59%	60.7%
N-OMC/SiO_2	[56]	200 mA/g /100/650 mAh/g	42%	~22%
BP-CS	[53]	200 mA/g /200/611 mAh/g	99.5%	77.4%
SiO_2-NT/G network	[57]	100 mA/g /100/1145.3 mAh/g	54.8%	44.9%
15-SiO_2@C-G	[58]	100 mA/g /216/542 mAh/g	47.6%	59.8%
SiO_2–CNFs	[55]	100 mA/g /30/231 mAh/g		90.2%
SiO_2@graphite	[54]	100 mA/g /100/433 mAh/g	66%	60.9%
C-mcms	[62]	500 mA/g /150/1055 mAh/g	~100%	>95%
Si—O—C	[63]	100 mA/g /40/>500 mAh/g	66.9%	~55.9%
Si/SiO_2@C (50 wt% C)	[64]	50 mA/g /100/482 mAh/g	59.9%	70.3%
nano-Si/a-SiO_2@C (33.4 wt% C)	[65]	750 mA/g /200/~800 mAh/g	72.5%	84.5%
Si@SiO_2/C	[66]	420 mA/g /200/1071 mAh/g	61%	42.7%
SiC@SiO_2-CSNWs	[67]	268 mA/g /100/~754 mAh/g	~15%	
pSS/CNTs	[68]	500 mA/g /200/1200 mAh/g	70%	~42%
Si@C@SiO_2	[70]	200 mA/g /305/880 mAh/g	73.2%	73%
Si@SiO_2/CNTs	[71]	500 mA/g /100/2035.9 mAh/g	86%	71.5%
SiO_2@Fe_3O_4@C	[52]	100 mA/g /100/140 mAh/g	62.7%	13.7%
SiO_2@NiO	[72]	100 mA/g /60/585 mAh/g	~60%	29.8%
2-SSZ	[73]	100 mA/g /30/461 mAh/g		37.3%
MSG250 (~42 wt% MoS_2)	[80]	100 mA/g /100/1060 mAh/g	~75%	~62%
Bi_2S_3@SiO_2	[81]	1000 mA/g /4000/379 mAh/g	~55%	55%

[a] CD: Current density.
[b] ICE: Initial coulombic efficiency.

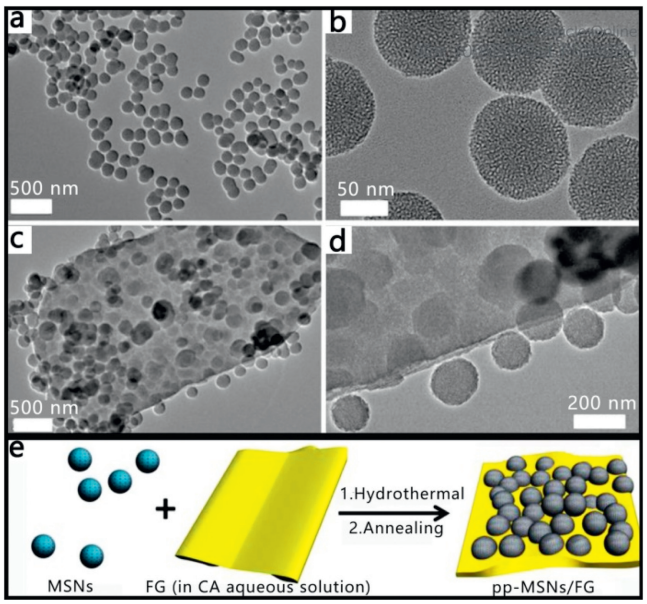

Fig. 2. (a, b) TEM images of MSNs with different magnification; (c, d) TEM images of pp-MSNs/FG; (e) the illustration of preparing pp-MSNs/FG nanocomposites. Reproduced with permission [50]. Copyright 2015, American Chemical Society.

rate performance, superior cycling stability and an extensible synthetic procedure for inexpensive starting materials makes BP-CS a likely negative electrode material in the market. Yin *et al.* [58] also prepared SiO_2@C-graphene composite materials with excellent electrochemical performance through self-assembly and ultrasonic-assisted hydrothermal and heat treatments. However, the self-assembly method has major problems in terms of yield and long-term consumption, so it has not been developed on a large scale to meet commercial needs.

In continuously improving the synthesis of SiO_2/C composites, scientists have proposed many new concepts and tried new methods. Hao *et al.* [59] proposed a dipping concept to prepare SiO_2-MC composites. During the experiment, amorphous SiO_2 was evenly inlaid in a tube rampart of mesoporous carbon. Then, with the absence of SiO_2 or carbon granules in the tube rampart, the SiO_2-MC composite electrodes exhibited a reversible capacity of 670 mAh/g, much higher than that of the electrodes containing SiO_2 congeries (SiO_2+MC; ~300 mAh/g). Zuo *et al.* [60] proposed the neoteric and reasonable idea of capturing Li in a microcage made of carbon nanotubes (CNTs) and porous SiO_2 sheaths to limit the depositional morphology and inhibit dendritic growth. With the dendritic growth inhibited, the electrode maintained a 99% electroplating/stripping effectiveness over 200 cycles. The results provided fresh opinions regarding the layout of Li metal anodes and accelerated the actual application of LIBs. To realize a simple and low-cost strategy, Cui *et al.* [41] prepared micron-sized porous C/SiO_2 composites from rice husks by a simple carbonization process (the synthesis process is shown in Fig. 3d). Jia *et al.* [61] synthesized nanofiber SiO_2-C composites by using filter paper as a scaffold and a carbon source.

In addition to innovations in synthesis, scientists have also tried to innovate in the product structure/composition. Beyond improvement of two-layer and two-phase SiO_2/C composites, researchers proposed the idea of synthesizing three-layer composites and multiphase composites based on SiO_2/C composites. Cao *et al.* [62] prepared a novel carbon-silica-carbon (C-mcms) three-layer structure of C/SiO_2 composites. Compared with similar non-carbon or carbon-shell composite electrodes, C-mcms composite electrodes have a high reversible capacity and good rate performance and cycling stability. The C-mcms electrode displayed a capacity of ~1055 mAh/g at 500 mA/g after 150 cycles without disintegration. In 2015, Xiao *et al.* [63] prepared Si/SiO_2/C composites with a high-temperature pyrolytic procedure. Firstly, phenolic resin, commercial nano-sized SiO_2 powder, flake graphite powder and SiO_2 sol were dissolved in absolute ethanol in that order, then evaporated and heated for 2 h under an argon atmosphere. Through various characterizations, it was found that the powdered Si/SiO_2/C composites had a diameter of approximately 1 μm, and the uniform pyrolytic carbon layer on the surface of the Si/SiO_2/C composites was approximately 5 nm thick. Moreover, it was found that the Si/SiO_2/C composites had minor electrochemical resistance and a superior Li^+ spreading rate by electrochemical impedance spectroscopy (EIS) measurement. Subsequently, Zhou *et al.* [64] synthesized Si/SiO_2@C composites

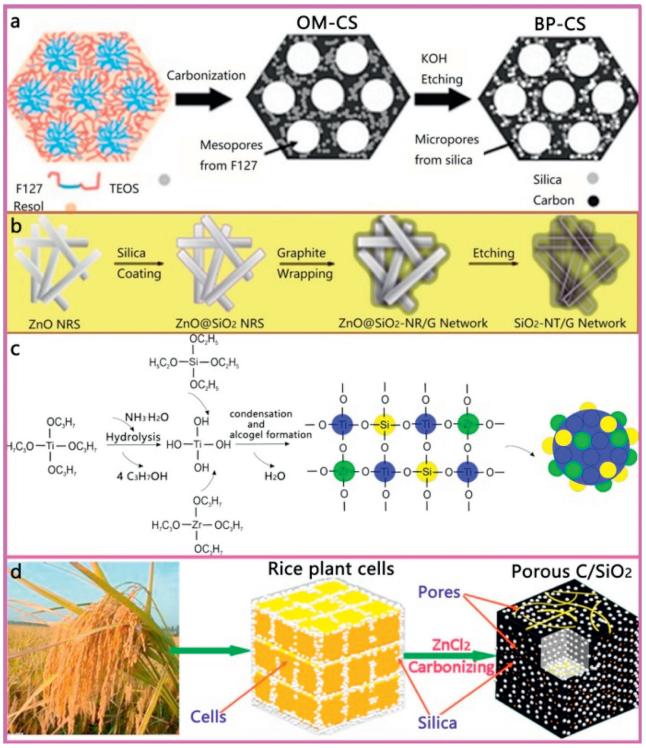

Fig. 3. (a) Diagrammatic sketch about the nanostructure development amid making of OM-CS and BP-CS. Reproduced with permission [53]. Copyright 2017, American Chemical Society. (b) Sketch map for the formation about SiO_2-NT/G network. Reproduced with permission [57]. Copyright 2015, Wiley. (c) The heterogeneous procedure about TiO_2-SiO_2-ZrO_2 oxide setup. Reproduced with permission [77]. Copyright 2017, ECS. (d) Fabrication process of C/SiO_2 composite. Reproduced with permission [41]. Copyright 2017, Elsevier.

in a simple and convenient way (mechanical grinding and a magnesium heat reduction process). The Si/SiO_2@C composites had excellent electrochemical properties (Fig. 4). In addition, compared to LIBs fabricated with SiO_2@C composites, the LIBs using Si/SiO_2@C composites as negative electrode materials exhibited superior capability and density. To improve the electrochemical performance of Si/SiO_2 composites, Fu *et al.* [65] designed, synthesized, characterized and tested a composite comprising nano-Si and amorphous SiO_2 (nano-Si/a-SiO_2) and carbon-coated nano-Si/a-SiO_2 (nano-Si/a-SiO_2@C) composites. The results showed that, compared with the Si/a-SiO_2 composites, the nano-Si/a-SiO_2@C composites demonstrated better reactivity dynamics and structure stability. From the synergistic effects of the carbon coating suppressing nano-Si cracking, the a-SiO_2 buffer layer reducing the bulk expansion and the 2D macrostructure, the flaky nano-Si/a-SiO_2@C anode exhibited superior cycle stability and good rate performance. After 300 cycles, the electrode showed only a volume expansion of 24%, small cracks and a capacity retention of 92% at 7.5 A/g. In 2018, Shen *et al.* [66] developed a new method to synthesize Si@SiO_2/C composites. Using a special uniform cellulosic liquid solution and inexpensive Si nanopowders as raw materials, the cellulosic Si material was assembled directly through *in situ* regeneration and then carbonized to obtain a Si/SiO_2/C composite with Si@SiO_2 uniformly encapsulated in a cellulose-derived carbon network. Similarly, since the SiO_2 buffer layer offered good buffering to the bulk expansion and the carbon supplied a highly conductive network for electrons, the Si/SiO_2/C composite electrode exhibited excellent electrochemical performance. After 200 cycles, the specific capacity reached 1071 mAh/g and the capacity retention reached 70% at 420 mA/g. With the deepening of research on the morphology of Si/SiO_2/C composites, composite forms other than the lamellar morphology are now known. For example, Hu *et al.* [67] prepared bead-shaped SiC@SiO_2 core-shell nanowires (SiC@SiO_2-CSNWs) on graphite paper (GP) through CVD; Su *et al.* [68] used magnesium steam thermal reduction to synthesize porous Si and SiO_2 (pSS) particles and *in situ* grown CNTs in pSS pores by CVD; Xiao *et al.* [69] synthesized 3D interconnected mesoporous C/Si/SiO_2 composites using SBA-15 as a Si source and CH_4 as a carbon precursor by two simple processes of magnesium thermal reduction and CVD; Yang *et al.* [70] synthesized a dual-core Si@C@SiO_2 composite electrode and

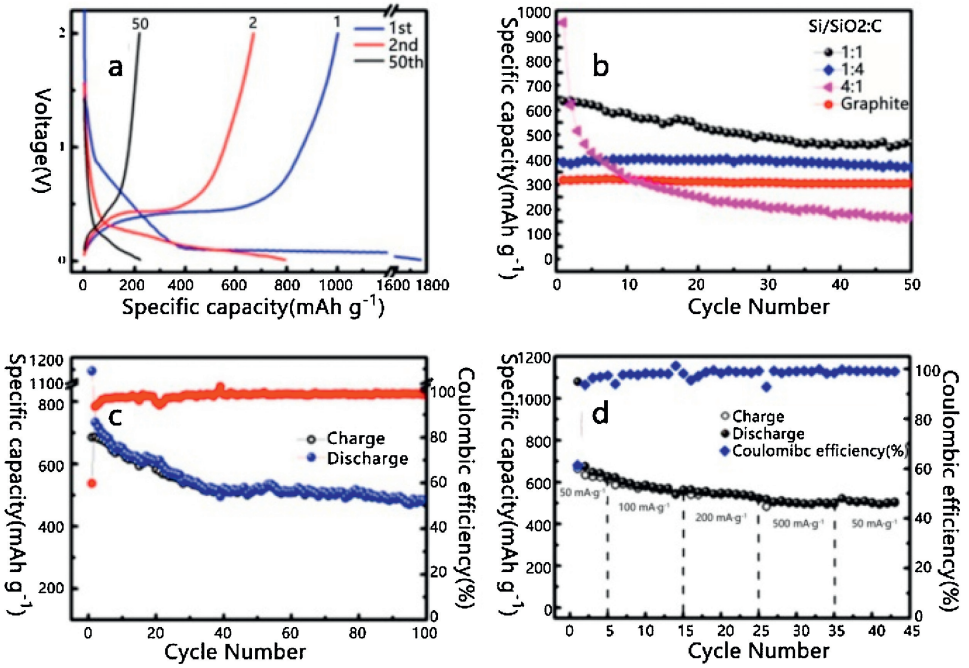

Fig. 4. (a) Discharge charge curves of Si/SiO_2@C (mass ratio, Si/SiO_2:C = 4:1) electrode at 50 mA/g and a voltage range of 0.01~2.0 V; (b) Cycling stability of a series of Si/SiO_2@C composites (mass ratio, Si/SiO_2:C = 1:1, 1:4, 4:1) at 50 mA/g; (c) Si/SiO_2@C (mass ratio, Si/SiO_2:C = 1:1) composites showed up the first discharge capacity of 685.8 mAh/g and 59.9% ICE; (d) Rate performance of the Si/SiO_2@C composites. Reproduced with permission [64]. Copyright 2015, Elsevier.

demonstrated its excellent cycling stability; and Wang *et al*. [71] synthesized Si@SiO_2/CNT composites consisting mainly of CNTs. Hou *et al*. [52] proposed a new idea of doping SiO_2/C composites with MO_x improve their electrochemical properties. A uniform core-shell SiO_2@Fe_3O_4@C composite was prepared by the hydrothermal method using SiO_2 nanospheres as templates. First, SiO_2 nanospheres and ferrocene were uniformly dispersed in acetone in that order. Then, hydrogen peroxide was dropped into the mixture and stirred for 3 h, and finally the mixture was moved into autoclave and kept at 220 °C for 24 h. The structure and electrochemical performance of the SiO_2@Fe_3O_4@C composites were characterized by modern analytical techniques. The research proved that SiO_2 nanospheres as a solid template avoid the aggregation of Fe_3O_4 nanoparticles (NPs). Furthermore, it was found that the SiO_2@Fe_3O_4@C composite electrodes had a high reversible capacity and a good cycling stability due to the presence of the mesoporous carbon layer, the sandwich multilayers structure and the Fe_3O_4 NPs. The SiO_2@Fe_3O_4@C composite electrodes achieved a capacity of 140 mAh/g after 100 cycles at 100 mA/g. Therefore, SiO_2@Fe_3O_4@C materials have broad application prospects, especially for LIBs.

2.2. SiO_2/MO_x composites

In SiO_2 crystals: since each Si atom is bonded to four O atoms and each O atom is in a tetrahedron composed of another Si atom, Si-O bonds each contain 1/2 covalent bond and ionic bond. In addition, due to the sp^3 hybridization of Si, the surrounding four Si-O bonds have the same bond energy, so that the crystal has a relatively stable structure. SiO_2 not only has the advantage of structural stability, but also has the disadvantage of poor electrical conductivity. The conventional crystalline SiO_2 material has poor electronic conductivity and is basically an electronic insulator, resulting in low electrochemical lithium storage activity as a negative electrode material. To this end, many approaches have been adopted to improve the lithiation/delithiation of SiO_2, such as the implementation of dendritic films, carbon-coated NPs and hollow nanostructures. However, in LIBs, those strategies do not substantially activate SiO_2 as an anode with strong Si-O bonds. Recently, some researchers studied the benefits of SiO_2 and metal-oxide composite materials as negative electrodes for LIBs. NiO, ZrO_2 and TiO_2 are the most commonly used MO_x materials complexed with SiO_2. The researchers compared the electrochemical properties of pure MO_x, pure SiO_2 and SiO_2/MO_x composites to discover the advantages of SiO_2/MO_x composites as anode materials for LIBs. From this research it can be judged whether MO_x can activate SiO_2 as an anode of strong Si-O bonds and the development prospects of SiO_2/MO_x composites can be evaluated.

In 2015, Wang *et al*. [72] synthesized SiO_2@NiO nanomaterials by assembling thin NiO shells with a radius of 40 nm *via* simple online sedimentation of NiO. By comparing the cyclic voltammetry (CV) results and electrochemical impedance spectra (EIS) of SiO_2, NiO and SiO_2@NiO electrodes, it was found that irreversible lithiation of SiO_2, while metal Ni NPs generated by the irreversible lithiation of NiO were responsible for the activation of SiO_2. For this reason, the specific discharge capacity of the SiO_2@NiO electrode maintained 585 mAh/g at 100 mA/g and a coulombic efficiency (CE) of ~100% after 60 cycles. It also displayed a good cycling stability and an excellent rate performance after the first several cycles. After demonstrating that the SiO_2@NiO composite had good electrochemical properties, the researchers began experimenting with different MO_x materials such as zirconia [72,73], and titanium oxide [39,74]. Choi *et al*. [75] reported a new type of anodic material SiO_2/ZrO_2 which had outstanding electrochemical performance. Later, Choi *et al*. [73] revealed the mechanism of SiO_2/ZrO_2 (SSZ) anode materials by electrochemical testing and the influence of various Si/Zr molar ratios (Si/Zr = 0.5, 1 and 2) on the properties of SiO_2/ZrO_2. SSZ materials with different molar ratios of Si/Zr (0.5, 1 and 2) were prepared according to reference [76]. Studies showed that 2-SSZ (Si/Zr = 2) has better electrochemical performance than the 0.5- and 1-SSZ (Si/Zr = 0.5 or 1). Unlike 0.5- and 1-SSZ, which have an overall crystal structure, 2-SSZ consists of an overall amorphous structure with crystal structure associated with the Zr-O-Si bonds. In 30 cycles, the 2-SSZ anode delivered a capacity of 461 mAh/g at 100 mA/g. Lee *et al*. [74] manufactured a SiO_2/TiO_2 composite film. Because TiO_2 and SiO_2 were evenly deposited on both sides of the composite film, a fully activated electrochemical surface area was produced. Due to the addition of Si and the porous TiO_2 structure, the SiO_2/TiO_2 composite anode exhibited at least twice the capacity of a typical TiO_2 anode and was very stable over 250 cycles. In addition, there were other discoveries: (1) as a result of the decrease in charge transfer resistance, the capacity increased slightly with further cycling; (2) since the active site of SiO_2 increased in the process of the interfacial electrochemical reaction, the internal resistance was lowered. Kurc *et al*. [39] prepared amorphous TiO_2-SiO_2 and SiO_2 NPs by emulsion method and then the amorphous TiO_2-SiO_2 and SiO_2 NPs were used as $Li_4Ti_5O_{12}$ anode additives. All samples were analyzed *via* SEM, and the particle size distributions (PSDs), porous structure parameters (low-temperature N_2 sorption) and galvanostatic charge–discharge parameters were measured. The oxide addition significantly influenced the structure, morphology, and electrochemical performance of the anode. The results revealed that a proper quantity of TiO_2-SiO_2 and SiO_2 could lower the electrochemical polarization of $Li_4Ti_5O_{12}$ and improve the electrochemical reaction dynamics of Li^+ insertion/removal. The sample with 3 wt% TiO_2-SiO_2 showed the best cycling performance, and the capacity retention was 99% and 92% under 1 C and 5 C, respectively, after 50 cycles.

From Table 1, the composite materials comprising MO_x and SiO_2 generally show improved electrochemical performance compared to pure SiO_2. This is true for the ICE of the SiO_2/NiO composite electrodes and the ratio of capacity retention of the SiO_2/TiO_2 composite electrodes. The overall electrochemical performance of SiO_2/TiO_2 is better. To date, some researchers have attempted to synthesize bimetal-SiO_2 compounds as negative LIB electrodes. Siwińska-Stefańska *et al*. [77] prepared a TiO_2-SiO_2-ZrO_2 (TSZ) oxide system (TiO_2:SiO_2:ZrO_2 mole ratio of 8:1:1) by the sol-gel method. The precursor liquids of TiO_2, SiO_2 and ZrO_2 were respectively dissolved in an organic solvent isopropanol to form a colloid, and then dried, and finally calcined to obtain a sample. The synthetic mechanism of the TSZ oxide system is shown in Fig. 3c. The compounds were analyzed based on PSD, form, crystal texture, surface components, porous architecture and thermostability. In addition, the applicability of the TSZ oxide system to negative LIB electrodes was assessed in a constant-current charging and discharging fashion. As a negative electrode material, the TSZ oxide system had a high specific capacity, a good rate performance and significantly enhanced cycling.

2.3. SiO_2/others

In addition to the use of carbon and MO_x, Si is also added to SiO_2. Evschik *et al*. [78] discussed the effect of the binder on the stable specific capacity and the CE of the negative electrode membrane for the nano-sized Si@SiO_2 structure. Novikov *et al*. [79] prepared a spherical nanosphere Si@SiO_2 composite with a nucleus-case structure and a mean radius of approximately 25 nm by plasma chemistry. Si@SiO_2 anodes were studied by SEM, XRD, XPS and TM. The action of the Si@SiO_2 anode composites during cyclical charging/discharging was investigated by EIS. The study found that, during the EIS lengthening cycle and primary charging, a

different chemical reaction proceeded synchronously with the electrochemical reaction, affecting the impedance of the loop. At the 5th cycle, the reversible capacity was stable and reached 850 mAh/g, and the reversible capacity was not significantly reduced up to 40 cycles. However, the electrode characteristics dropped sharply after 40 cycles. The main cause was a solid product layer with a lower conductivity taking shape on the Si@SiO_2 granules, which finally caused a reduction in the anode discharge capacity.

In view of the excellent electrochemical performance of the SiO_2/MO_x composite materials, metal sulfides (MS_x) have also been explored in this pursuit. Research found that, due to the good electrical conductivity, high energy density and theoretical specific capacity and low cost of MS_x, the electrochemical properties and future development of SiO_2/MS_x composites are more promising than those of SiO_2/MO_x composites. Tang *et al*. [80] first designed and synthesized a novel Bi_2S_3@SiO_2 core-shell-type microwire. Although the bulk expansion of Bi_2S_3 was large and the cycle performance was poor, the mechanical rigidity of the shapeless SiO_2 could reduce the bulk expansion. The Bi_2S_3@SiO_2 composite showed exceptional electrochemical performance, such as a massive cycling longevity and a high capacity. After 4000 cycles, the discharge capacity was 379 mAh/g at 1 A/g. Han *et al*. [81] proposed a new strategy for preparing MoS_2/SiO_2/G hybrids (MSGs). Monodisperse MSGs were prepared by hydrothermal synthesis of MoS_2 on SiO_2-modified G sheets (SGs) and followed by pyrolysis under a nitrogen atmosphere. Since the inert SiO_2 in the hybrid can effectively mediate the volume expansion of MoS_2 in the lithiation process, the MSG electrodes with ~ 42 wt% MoS_2 expressed a 1060 mAh/g stable capacity at 0.1 A/g over 100 cycles. In addition, the electrode retained a specific capacity of 580 mAh/g at 8 A/g.

3. SiO composites

SiO is not a naturally existing substance. It is made by reacting SiO_2 with Si, and the synthesis is expensive. Therefore, SiO is the least used composite material in SiO_x-based composites. However, because of the special nature of the SiO synthesis, synthesized SiO composites have their own unique properties (as shown in Table 2).

3.1. SiO/C composites

Carbon is often added in the form of a carbon coating or carbon doping. Due to the addition of carbon, the resultant composite has better electrical conductivity, a slow volume change and good electrochemical performance.

In 2007, Kim *et al*. [37] synthesized SiO-C composites using ball milling and pyrolysis. For the preparation of the SiO-C composite powder, first, pure SiO powder was ground for 12 h under an argon atmosphere and polyvinyl alcohol (PVA) was dissolved in deionized water. Then, the two were uniformly mixed and pyrolyzed in an Ar atmosphere for 2 h. The samples were characterized *via* SEM (Figs. 5a and b), XRD (Fig. 5c), and HRTEM (Fig. 5d). As a result, it was found that the anode material had a first charge and discharge capacity of ~1050 and 800 mAh/g, respectively, and had an ICE of 76%. The composites exhibited a reversible capacity of 710 mAh/g for 100 cycles with no latent or capacity limit. Kim *et al*. [82] prepared SiO_2-C anode materials by the Si cation chelation method. The SiO_2-C composite had submicron granules and a distinct hollow globular microstructure that gave it a high cycling stability. At the 100th cycle, it delivered a capacity retention of 91%, a discharge capacity of 662-602 mAh/g, and a CE of 99.8%. Yuan *et al*. [83] prepared SiO/reduced G oxide (SiO/rGO) composites *via* the hydrothermal method, which involved encapsulating SiO particles with a G hydrogel and HF treatment. In the hydrothermal process, SiO granules scattered uniformly in the rGO substrate at the expense of the G hydrogel structure. The novel structure of the SiO/rGO composite played a key role in electrochemical performance. The composites exhibited a discharge capacity of 744 mAh/g at 120 mAh/g after 50 cycles. Shi *et al*. [84] synthesized vertical G-encapsulated SiO (d-SiO@vG) composites by a CVD method in which vertical G (vG) nanosheets grew directly on SiO particles. The composites not only improved the cycling stability of the high-quality loaded SiO anode but also

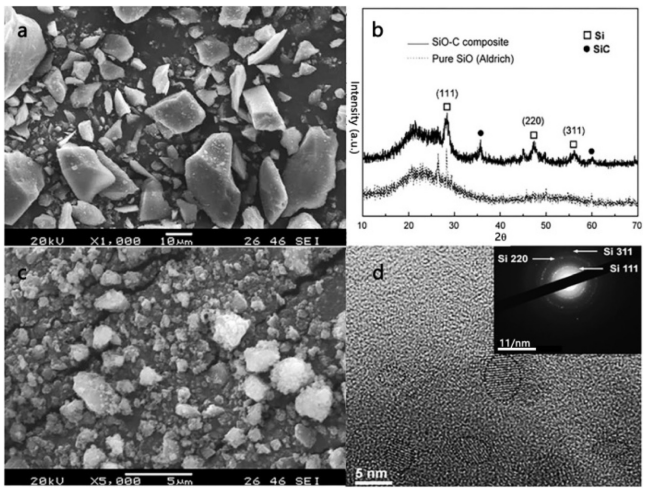

Fig. 5. (a) SEM graphs of pure SiO; (b) SEM graphs of ball milling SiO powders; (c) XRD maps of pure SiO and SiO-C composite powders; (d) HRTEM graphics and opted region diffraction map of SiO-C composites. Reproduced with permission [37]. Copyright 2007, Elsevier.

Table 2
Electrochemical properties of SiO composites in half-cell testing.

Anode material	References	CD[a] /Cycles/Cycle stability capacity	ICE[b]	Capacity retention
SiO-C	[37]	100 mA/g /100/710 mAh/g	76%	88.75%
F-SiO/H-rGO	[83]	120 mA/g /50/744 mAh/g	~68%	~41%
d-SiO@vG	[84]	1 C/400/~2500 mAh/g		~80%
SiO/G/CNTs&CNFs	[85]	100 mA/g /100/672.3 mAh/g	53.3%	~67%
HB-SiO	[42]	0.5 C/100/ 947 mAh/g	65.1%	52.5%
NC-SiO	[86]	1500 mA/g /200/955 mAh/g	73.9%	92.0%
mp-SiO@N-doped C	[87]	400 mA/g /250/806 mAh/g	65.7%	67.1%
LMP-SiO-C	[88]	0.5 mA/cm^2 /50/1500 mAh/g	71.8%	~85%
W@SiO-graphite	[89]	0.5 C/100/358 mAh/g	59.3%	63.2%
TC-SiO	[90]	700 mA/g /450/400 mAh/g		~40%
C-coated SiO/ZrO_2	[91]	800 mA/g /100/721 mAh/g	66.58%	~56%

[a] CD: Current density.
[b] ICE: Initial coulombic efficiency.

increased the postcycle retention and increased the energy density. Li *et al*. [85] also synthesized intercalated SiO/graphite/C nanotubes and C nanofibers (SiO/G/CNTs and CNFs) composites by high-energy wet ball milling, spray drying and CVD methods.

Some researchers doped nonmetallic elements in the C layer and then in the composites with SiO to improve the electrochemical properties of the SiO/C composites. Lee *et al*. [86] used nitrogen-containing ionic liquids to coat nitrogen-doped carbon layers on SiO particles to synthesize NC-SiO composites. Due to the N doping on the surface of the carbon coating layers improving the inherently moderate conductivity of the SiO anodes, N-doped carbon-coated SiO showed significantly improved cell performance compared to conventional carbon coatings, especially in specific capacity and magnification performance. Huang *et al*. [87] prepared multichannel porous SiO@N-doped carbon rods *via* a combination of electrostatic spinning and thermal treatment with the assistance of PMMA. The mp-SiO@N-doped carbon rod composite showed good cycling stability and rate performance due to its unique structure. At 400 mAh/g, a discharge capacity of 806 mAh/g was maintained after 250 cycles. Hideyuki Morimoto *et al*. [88] studied the performance of a carbon-coated SiO (SiO-C) electrode material containing a small amount of olivine-type $LiMgPO_4$ powder as an additive. It was found that the SiO-C anode containing 2 wt% $LiMgPO_4$ (LMP) exhibited a 1500 mAh/g charge-discharge capacity and good cycle performance and thermal stability.

More and more researchers are working on coating metal layers or metal oxide layers on SiO/C composites to improve their electrochemical properties. Yom *et al*. [89] coated tungsten (W) on SiO-graphite composites *via* the physical vapor deposition (PVD) method. The homogeneity of the coat determined by electron probe microanalysis was confirmed by TEM images. Because W coatings have excellent conductivity and mechanical properties, W-coated SiO-graphite composite electrodes have a higher reversible capacity and capacity retention rate than SiO-graphite composite electrodes. After 100 charging and discharging cycles, the electrodes showed a retention capacity of 63.2%, which was 11.2% higher than that of the SiO-graphite electrode. After 50 cycles, because of Si expansion, fissures were observed in the uncoated SiO-graphite electrode, whereas the surface of the W-coated SiO-graphite electrode had no damage. Dou *et al*. [90] synthesized TiO_2-C-SiO by incorporating 3% TiO_2 into a C-SiO complex. Analysis of the SEM and HRTEM images revealed that the introduction of 3% TiO_2 greatly improved the ordered carbon coating array of C-SiO, as shown in Figs. 6a-d. The TC-SiO composites with 3% TiO_2 exhibited noticeable merits in cycling stability and charging/discharging rate and an interfacial stability contrasting with that of the C-SiO composites. Another multicomponent composite (C-SiO/ZrO_2) made from SiO, carbon, MO_x was synthesized by Fan Cheng *et al*. [91] The C-coated SiO/ZrO_2 composites were prepared by combining high-energy ball milling with constant pressure CVD. Electrochemical analysis showed that the composite had excellent electrochemical properties, including a high initial discharge capacity (1737 mAh/g) and a significant cycling stability (reversible capacity of 721 mAh/g at 800 mA/g, after 100 cycles).

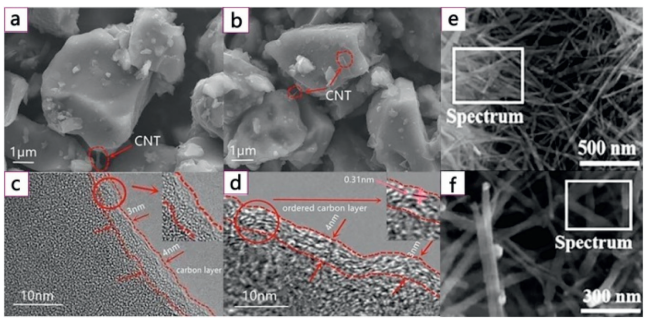

Fig. 6. (a,b) SEM graphics of C-SiO and 3% TC-SiO; (c,d) HRTEM graphics of C-SiO and 3% TC-SiO; (e) SEM graphics of SiO_x NWs; (f) SEM graphics of pC-SiO_x NWs. (a–d) Reproduced with permission [90]. Copyright 2018, Elsevier. (e, f) Reproduced with permission [106]. Copyright 2017, Royal Society of Chemistry.

3.2. SiO/others

In addition to SiO/C composites, nitrogen-doped SiO and SiO/MO_x are often synthesized to improve the electrochemical performance of SiO. Jeong *et al*. [92] synthesized TiO_2-coated SiO in an organic solvent anhydrous ethanol applying a simple sol-gel method and used various analytical methods to characterize the coated and uncoated SiO. Compared to uncoated SiO, TiO_2-coated SiO increased the ICE and reversible capacity, leading to a 30% addition of volumetric energy density. In addition, TiO_2 coatings can inhibit high-speed exothermic reactions, which can delay thermal runaway and reduce safety issues. Woo *et al*. [42] synthesized B-doped SiO anode materials with a one-step procedure consisting of heat disproportionation and impurity adulteration. The results showed that B-doped SiO obviously improved the internal resistance, rate performance and cycling capability of the electrode compared with SiO. The B-doped SiO electrode achieved a high capacity of 700 mAh/g or more at the 2C rate, which was approximately 3 times higher than that of pure SiO. Because Si has a large volume expansion and a high cost, there is less literature on the synthesis of SiO/Si composites. However, Yamano *et al*. [93] developed a high-capacity LIB with SiO-Si composite anodes and LR-NMC cathodes in 2005. SiO-Si composites were formed by applying SiO and Si powders as raw materials and powdered KB and PI resin as binders. This LIB can use the irreversible capacity of the positive electrode to compensate for the irreversible capacity of the negative electrode. Therefore, the battery shows excellent electrochemical performance, including excellent temperature performance, good capability, cycling stability and high safety.

4. SiO_x ($0 < x < 2$) composites

The composites formed by the combination of SiO_x ($0 < x < 2$) with different materials (such as C, Si, MO_x) will exhibit different electrochemical properties. Even if SiO_x is compounded with the same material, the electrochemical properties exhibited in the application of lithium ion batteries are different due to the different oxygen content in SiO_x (as shown in Table 3).

4.1. SiO_x/C composites

In the synthesis of SiO_x/C composite materials, the heat treatment method is the most common. Li *et al*. [94] synthesized a novel G nanosheet-supported SiO_x disordered carbon composite (SiO_x-C/GNPs) by heat treatment. Because SiO_x-C/GNPs have good electronic conductivity, short transport lengths of Li^+ and electrons and elastomer-like volumetric variations in the insertion/extraction of lithium and between SiO_x and GNPs, this new material has excellent electrochemical properties, including outstanding cycling stability and rate performance. After 250 cycles, a ~630 mAh/g steady reversible capacity was achieved and the capacity maintenance was nearly 100% at 100 mAh/g. Sun *et al*. [95] synthesized SiO_x/C NP composites by a simple thermopolymerization process and subsequent heat treatment. Because the carbon skeleton can offer a continuous network and ultrafine SiO_x NPs can reduce mechanical strain and shorten the diffusion/transmission distance of Li^+ and electrons, SiO_x/C NP

Table 3
Electrochemical properties of SiO_x composites in half-cell testing.

Anode material	References	CD[a]/Cycles/Cycle stability capacity	ICE[b]	Capacity retention
$SnSiO_{x+2}$@G-250	[125]	200 mA/g /200/1164 mAh/g	74%	~65%
2 wt%TiO_{2-x}@Si/SiO_x	[43]	200 mA/g /100/1140.9 mAh/g	52.2%	98.1%
Si-SiO_x-Al_2O_3	[126]	100 mA/g /50/731 mAh/g	65.7%	58.6%
Si-SiO_x-Nb_2O_5-C	[127]	500 mA/g /200/800 mAh/g		~89%
SiO_x-C/GNPs	[94]	100 mA/g /250/630 mAh/g	~65%	~70%
SiO_x/C NPs	[95]	500 mA/g /200/540 mAh/g	44.4%	37%
SiO_x/MWCNT/N-doped C	[96]	100 mA/g /450/621 mAh/g	~66%	~57%
porous SiO_x@C	[107]	100 mA/g /200/1230 mAh/g	45.04%	39.7%
SiO_x/C/G	[97]	200 mA/g /600/541 mAh/g	85.2%	76.7%
Ms-1300	[98]	100 mA/g /100/840 mAh/g	56%	~73%
SiO_x-C	[100]	100 mA/g /100/674.8 mAh/g	~70%	~56%
SiO_x/C	[99]	0.5 C/500/580 mAh/g	82.2%	73.9%
$SiO_{1.39}$-C	[101]	——/20/426 mAh/g	45.6%	45.2%
SiO_x/N-doped C	[102]	100 mA/g /100/1514 mAh/g	65%	~62%
SiO_x/C	[103]	100 mA/g /100/780 mAh/g	61%	56.5%
SiO_x/C	[104]	300 mA/g /200/843.5 mAh/g	65.7%	65.1%
nano-Si@SiO_x/graphite	[120]	100 mA/g /70/1560 mAh/g	~73%	~71%
pC-SiO_x NWs	[106]	500 mA/g /150/623 mAh/g	~50%	~57%
porous Si/SiO_x	[108]	600 mA/g /560/1503 mAh/g	43%	33.4%
Si/SiO_x	[109]	1000 mA/g /500/915 mAh/g	~60%	~44%
PED-Si/SiO_x-1%	[111]	200 mA/g /80/968.2 mAh/g	46.2%	~98%
vesicular Si@SiO_x-SiO_2	[112]	60 mA/g /50/~200 mAh/g	37%	
Si/SiO_x/SiO_2	[40]	200 mA/g /350/~600 mAh/g		
Si@u-SiO_x@GNSs	[114]	200 mA/g /50/1844.9 mAh/g	81.5%	62.9%
Si@SiO_x@C	[115]	1000 mA/g />500/>1030 mAh/g	77%	~52%
SNs@SiO_x/C	[116]	400 mA/g /300/779 mAh/g	68.3%	95.8%
Si/SiO_x@C	[117]	400 mA/g /200/1023 mAh/g	63.6%	~47%
Si-SiO_x-C	[118]	1 C/200/1034.6 mAh/g	80.2%	77.6%
Si@SiO_x@22.45 wt% C	[38]	100 mA/g /150/1051 mAh/g	71%	~66%
Si@SiO_x/CNTs@C	[119]	420 mA/g /700/1740 mAh/g	58.4%	58.6%
Si@SiO_x/29% GH	[121]	100 mA/g /140/1640 mAh/g	53%	~30%
c-nSi/SiO_x@$C_{4.0}$	[123]	1000 mA/g /500/>850 mAh/g	85.53%	~45%
Si/SiO_x-C	[124]	100 mA/g /50/1644 mAh/g	76%	85.4%
Si@SiO_x/Ni/graphite	[129]	100 mA/g /100/742.3 mAh/g	65.3%	35%

[a] CD: Current density.
[b] ICE: Initial coulombic efficiency.

composites have superior electrochemical performance. The prepared composite electrodes showed a high reversible capacity of 540 mAh/g at 500 mA/g after 200 cycles. Ren [96] and Xu [97] also synthesized SiO_x/C composites by heat treatment.

The sol-gel method integrated with heat treatment is also a common synthesis method for SiO_x/C composites. Lv *et al.* [98] synthesized SiO_x-C dual-phase glass composites as a negative LIB electrode *via* a simple sol-gel method. The solution containing the silicon source was completely dissolved in an organic mixed solution of ethanol, citric acid and ethylene glycol, and then gelled, followed by aging and drying, and finally heat treatment at different temperatures. The SiO_x-C composites obtained at 1000 °C, 1200 °C, 1300 °C and 1400 °C were studied and compared. The SiO_x-C composite obtained at 1300 °C had the best electrochemical performance. At 100 mA/g, the composite offered a high reversible capacity of 840 mAh/g and excellent rate performance through 100 cycles. It was found that the excellent electrochemical performance of the SiO_x-C biphasic glass electrode could be attributed to the following: (1) a distinct two-phase glass construction, in which shapeless SiO_x phase was uniformly scattered and in intensive contact with nanoscale free carbon components; (2) a SiO_x phase with a low specific value of O/Si; (3) good contact of the unrestrained carbon supplying good conductivity for the electrode reaction; and (4) the unrestrained carbon constituents relieving bulk expansion in the process of discharging/charging. Xu *et al.* [99] and Wu *et al.* [100] also synthesized SiO_x-C composites by the sol-gel method.

Other methods are also commonly used by researchers, such as evaporation and reduction (magnesithermal reduction, alumino-thermic reduction). Cheon *et al.* [101] synthesized a dense micrometer-sized $SiO_{1.39}$-C composite by $SiO_{1.39}$ NPs that were prepared by an evaporation method using phenolic resin and a conductive carbon composite. According to the results of the structural analysis, no structural changes occurred during the heat treatment at a temperature below 1000 °C. From the microstructure analysis, dense particles with sharp edges were obtained when the annealing temperature was over 800 °C. The test found that the CE of the composite increased from 93.6% to 97.5% in the 5th cycle and proceeded to grow with each added cycle. In addition, it was found that the composites annealed at 1000 °C enabled a specific capacity of 426 mAh/g and a CE of 99.7% at the 20th cycle. Shi *et al.* [102] synthesized nucleus-case SiO_x/N-adulterated carbon composites by a relatively simple thermal evaporation method and carbonization process. The N-adulterated carbon layer guaranteed excellent electrochemical performance for the SiO_x/C composites. After 100 cycles, the layer enabled a reversible capacity of 1514 mAh/g at 100 mA/g and 933 mAh/g at 2A/g, respectively.

With the progress of science and technology, many experiments have to sought to reduce the cost of synthesis and improve the electrochemical performance of SiO_x/C composites. Researchers have proposed many new composite structures, synthetic ideas and synthesis methods. Gao *et al.* [103] proposed a new method (a template-assisted solvothermal method combined with carbon coat crafts) to synthesize SiO_x/C composites that had mesoporous structure, a pore magnitude distribution of 2–4 nm and a high specific surface area. The evenly arranged mesoporous and thin-walled holes of the SiO_x/C composites guaranteed rapid electrode reactions and provided a self-buffering effect in the charging and discharging process. Therefore, the SiO_x/C anode showed superior electrochemical performance, such as a high specific capacity

(780 mAh/g), excellent cycling stability (0.02% decay per cycle), and a good rate performance. Zhang *et al.* [104] synthesized microcrystalline SiO_x/C core-shell composites by a simple and efficient method of carbonizing citric acid and ball milling SiO_x blends. For the preparation of the composites, first, ball-milled SiO_x powder (for a detailed preparation see reference [105]) and citric acid were thoroughly mixed in absolute ethanol and then dried to remove the ethanol. Finally, the mixture was annealed at 600 °C for 4 h under a N_2 atmosphere. The C layer obviously improved the conductivity of SiO_x and extenuated the bulk changes of SiO_x in the process of lithiation and delithiation. The SiO_x/C composites exhibited a CE of 99.8% and a capacity retention of 65.1% (the reversible capacity was 843.5 mAh/g) after 200 cycles. A novel routine was developed for the preparation of nano Si@SiO_x composites. Using low-cost mesoporous SiO_2 spheres, Li *et al.* [106] synthesized core-shell carbon-coated SiO_x NWs (pC-SiO_x NWs) as a new LIB anode *via* a novel self-sacrificing method. By comparing the SEM images of the SiO_x NWs and pC-SiO_x NWs, it was showed that the synthesized pC-SiO_x NWs had oxygen vacancies (Figs. 6e and f). Consequently, the composites showed excellent cycling stability with a high reversible specific capacity of 1060 mAh/g (100 cycles) and 623 mAh/g (150 cycles) at 100 mA/g and 500 mA/g, respectively. To meet the low-cost, simple synthesis and clean and pollution-free requirements, Cui *et al.* [107] synthesized a micronized multiaperture SiO_x@C composite by aluminum heat reduction using paddy husks as raw materials.

4.2. SiO_x/Si composites

Among the various means to improve the electrochemical properties of SiO_x, adding a coating to the surface is one of the most common approaches. In addition to the most common carbon coatings, silicon coatings are being studied by more and more scientists. Hen *et al.* [108] synthesized porous Si nanowires *via* a metal-aided chemical etching method using inexpensive metallurgical Si as a raw material. Interestingly, a thin SiO_x layer ($\sim$ 3 nm) took shape on the exterior of the porous Si nanowires and steadied the cycle capability of the LIB. The study found that the composites could provide a 1503 mAh/g reversible capacity in the 560th cycle at 600 mA/g, and each cycle was reduced by $\sim$0.04% compared to the initial capacity. Chen *et al.* [109] prepared a creative Si/SiO_x porous structure with different thicknesses of SiO_x coatings by a simple annealing and pickling process. Analogously, the Si/SiO_x porous structure exhibited improved electrochemical performance due to the addition of the SiO_x coating. The structure enabled a high reversible discharge capacity of more than 915 mAh/g at 1 A/g after 500 cycles. Lee *et al.* [110] synthesized four distinct proportions of NPs that consisted of a crystalline Si core and an amorphous SiO_x shell using microwave-generated plasma. It was concluded that a 20% SiO_x shell was the best in terms of electrochemical performance. The material enabled an initial capacity of 2030.34 mAh/g, an ICE of 64.41%, and a capacity retention of 79.92% in the 50th cycle.

To further improve the electrochemical performance of the Si/SiO_x composites, researchers synthesized new substances. Park *et al.* [111] synthesized Si/SiO_x-PEDOT:PSS core-shell structured materials using the conductive polymer poly(3,4-ethylenedioxythiophene):poly(4-styrenesulfonate) (PEDOT:PSS). Somodi *et al.* [112] synthesized another multilayer hybrid bubble Si@SiO_x-SiO_2 composite by pyrogenic hydrogen silsesquioxane. Dai *et al.* [40] synthesized Si/SiO_x/SiO_2 nanocomposites by a simple and extensible chemical method. Due to their unique nanostructure, the composites showed a high capacity of 600 mAh/g and a 99% CE for more than 350 cycles. Bae *et al.* [43] proposed a new idea: adding MO_x to Si/SiO_x composites. Therefore, the TiO_{2-x}-coated Si/SiO_x nanospheres (TiO_{2-x}@Si/SiO_x) were synthesized. TiO_{2-x}@Si/SiO_x composites have many improved properties, including CE and heat stability, compared to Si/SiO_x nanosphere anode materials. The TiO_{2-x}@Si/SiO_x nanosphere negative electrode displayed a 1200 mAh/g reversible capacity and excellent cycling stability.

However, the addition of carbon coating or carbon doping is the most common method to improve the electrochemical performance of Si/SiO_x composites. In 2008, Hu *et al.* [113] synthesized a Si@SiO_x/C nanocomposite solution *via* hydrothermal carbonization of dextrose in the presence of Si NPs. For the preparation of the composite, Si NPs (20–50 nm) were firstly dispersed by sonication in water in an autoclave. Then, glucose was added to the dispersion, and the mixture was thermally treated for 12 h under 200 °C. Finally, the above mixture was centrifuged and then further carbonized at 750 °C for 4 h under N_2. Heat treatment is one of the common methods for synthesizing Si@SiO_x@C composites and often involves ball mills and CVD. Niu *et al.* [114] prepared G nanosheets (GNS) encapsulated with ultrathin Si@SiO_x by self-assembly and heat treatment. NH_2-terminated Si NPs with ultrathin SiO_2 were effectively acquired by a one-step reaction in an ammonia-water-ethanol mixture. Due to the ultrathin SiO_x on the Si NPs and the good GNSs encapsulation structure, the Si@u-SiO_x@GNSs acquired by self-assembly and thermal reduction exhibited superior performance. The material enabled a reversible capacity of 2391.3 mAh/g and reached a 1844.9 mAh/g capacity after 50 cycles at 200 mA/g. Jiang *et al.* [115] first milled SiO_2 fume and then pyrolyzed a polymethylmethacrylate (PMMA) polymer directly on Si NPs to fabricate a dinuclear Si@SiO_x@C nanocomposite. As a result of their distinct double-nucleus shell construction, the nanocomposites exhibited a stable cycling performance. The material enabled a capacity of up to 1972 mAh/g, and the capacity was approximately stable at 1030 mAh/g over 500 cycles. Sun *et al.* [116] synthesized SiO_x and carbon bilayer-coated Si nanorods (SNs@SiO_x/C) by etching Si-Al alloy microspheres followed by thermal vapor deposition. The dual-layer structure of the native SiO_x and the carbon availably controlled the volume expansion of the SNs, avoiding exposure to the electrolyte and enhancing the electronic conductivity. Therefore, the SNs@SiO_x/C composites enabled superior electrochemical performance. Over 300 cycles, the composites reached a reversible capacity of 779 mAh/g at 400 mA/g, retaining 95.8% of the initial capacity. Zhu *et al.* [117] integrated Si/SiO_x@C composites by low-temperature molten salt reduction and pyrolysis. Lee *et al.* [118], Zhang *et al.* [38] and Li *et al.* [119] also synthesized Si-SiO_x-C composites, nano-Si@SiO_x@C composites and Si@SiO_x/CNTs@C composites on the basis of heat treatment techniques.

Gu *et al.* [120] adopted a new method to synthesize Si@SiO_x/graphite composites. Nano-Si@SiO_x was produced from SiO_2 by a combination of electrolysis and delamination techniques and then used as a precursor to synthesize nano-Si@SiO_x/graphite composites. The study found that the synthesized nano-Si@SiO_x/graphite composite led to a steady discharge capacity and good cycling stability and rate performance. Bai *et al.* [121] successfully synthesized Si@SiO_x/G hydrogel (GH) composites *via* a self-assembly method. Due to the multi aperture 3D fabric of the GH and the conductive G matrix, the Si@SiO_x/GH composite had excellent electrochemical properties. The Si@SiO_x/GH electrode containing 71 wt% Si@SiO_x exhibited a high capacity of 1640 mAh/g after 140 cycles at 0.1 A/g. Qian *et al.* [122] proposed a simple and inexpensive two-step ball milling method to prepare Si/SiO_x/C composites using commercial SiO and graphite. Because of the synergism of the Si/SiO_x phase and graphite, the Si/SiO_x/C electrode showed a high capacity of 726 mAh/g and a capacity retention of 82% after 500 cycles at 0.1 A/g.

Since adding an amorphous carbon coating to Si/SiO_x is a common method to improve the rate performance of Si/SiO_x, some studies [123,124] have reported that the content of the carbon coating, the growth time of the carbon coating and other factors

have a great effect on the electrochemical performance of the composites. To this end, many scientists have conducted in-depth research. Zhuang *et al.* [123] synthesized coral-shaped nanostructured Si composites (c-nSi/SiO_x@C_y) by combining a sulfuric-acid-etched $Al_{60}Si_{40}$ alloy with surface-grown carbon coating technology. The study found that c-nSi/SiO_x@C_y composites containing 4.0 wt% carbon (c-nSi/SiO_x@$C_{4.0}$) showed the best electrochemical performance. The c-nSi/SiO_x@$C_{4.0}$ electrode had an ICE of 85.53% and a specific capacity of 2200 mAh/g at 0.1 A/g for voltages of 0.01 ~1.5 V. The electrode could maintain a high specific capacity of 1600 mAh/g after 50 cycles at 0.1 A/g. Hoeltgen *et al.* [124] also synthesized Si/SiO_x-C nanocomposites by surface-grown carbon coating techniques and examined the influence of carbon growth on the amorphous SiO_x layers using different carbon coating times. In addition, the effect of gradual carbon growth on the electrochemical performance was also studied. Finally, the best electrochemical performance was obtained at 40 min of carbon plating. At 500 mA/g, the reversible capacity was over 2100 mAh/g, the ICE was more than 75%, the capacity retention was 84% and the cycle capability was as high as 50 cycles.

4.3. SiO_x/MO_x composites

To further improve the electrochemical performance of SiO_x/MO_x composites, some scientists tried various synthetic methods and also tried to add coatings. Common coatings are carbon coatings and Si coatings. Other researchers attempted to embed carbon and Si in SiO_x/MO_x composites.

He *et al.* [125] synthesized $SnSiO_{x+2}$@G-250 ($1.29 \leq x \leq 1.71$) nanofibers. They first synthesized nanofibers comprising $SnCl_2$, TEOS and PVP and then successfully grew ultrathin graphite carbon on the surface of $SnSiO_{y+2}$ nanofibers using CVD. The obtained $SnSiO_{x+2}$@G-250 nanofibers had two distinct advantages: (1) a unique hierarchical carbon framework of continuous surface carbon graphite and a core carbon network; and (2) atomic-level SnO_x in the dispersed core. As a result, this novel $SnSiO_{x+2}$@G-250 nanofiber could be used directly as an adhesive-free LIB electrode, showing either a high specific capacity (~1150 mAh/g) or good cycling stability (a capacity retention of ~100% at 0.1 A/g after 200 cycles).

In contrast to the above coating method, Kim *et al.* [126] synthesized nanocrystalline Si-embedded SiO_x-Al_2O_3 composites by high-energy mechanical ball-milling means and researched their potential as negative electrode materials for LIBs. In the process of ball milling, SiO_2 was partially reduced, Al was simultaneously oxidized into Al_2O_3, and the resulting nano-Si was embedded in the SiO_x-Al_2O_3 composites. The composite was analyzed *via* XRD, Raman spectroscopy, XPS and HRTEM. In the electrochemical tests, the composite electrode had a reversible capacity of ~850 mAh/g, and an ICE of 66%. Kim *et al.* [127] used Si and Nb_2O_5 micron-sized powders as starting materials and synthesized nanosilica-embedded SiO_x-Nb_2O_5-C composites *via* high-energy mechanical milling (HEMM). For the material preparation, Si, Nb_2O_5, and activated carbon powders were placed in proportion into a steel cylinder and then subjected to HEMM treatment under an Ar atmosphere. The composites were analyzed by SEM, TEM and XRD (Fig. 7). Moreover, it was found that some chemical changes during the ball milling process: (1) Si granules gained oxygen from Nb_2O_5 to form SiO_x; (2) nano-Si became embedded in the formed SiO_x; and (3) Nb_2O_5 was partially reverted. Additionally, because of these changes, the SiO_x-Nb_2O_5-C composite electrodes exhibited excellent electrochemical performance with a reversible capacity of ~800 mAh/g for 200 cycles.

4.4. SiO_x/others

Compositing with metals can also improve the electrochemical performance of SiO_x. A large part of the first irreversible specific capacity of SiO_x is caused by the first inert Li_2O and lithium silicates. The ICE of the composite electrodes can be effectively improved by preforming the MO_x or silicates in combination with SiO_x. At the same time, the formed oxides or silicates can produce volume expansion during lithium intercalation of the buffer material, which is beneficial to the cycle performance of the material, and the excess or partially unoxidized metal can also improve the conductivity of the overall material. Tashiro *et al.* [128] produced nanocomposite SiO_x-Ti powder *via* PVD. As the amount of Ti increased, it was found that the formation of titanium silicide became notable compared with the oxidation of Ti, which easily led to a reduced amount of activated Si and hence a significant reduction in capacity. To remedy this, several studies have attempted to develop multilayer mixtures by recombining other phases on the basis of SiO_x-M. Wang *et al.* [129] prepared ternary-grade SiO_2-Ni-graphite composites *via* two-step ball milling. Due

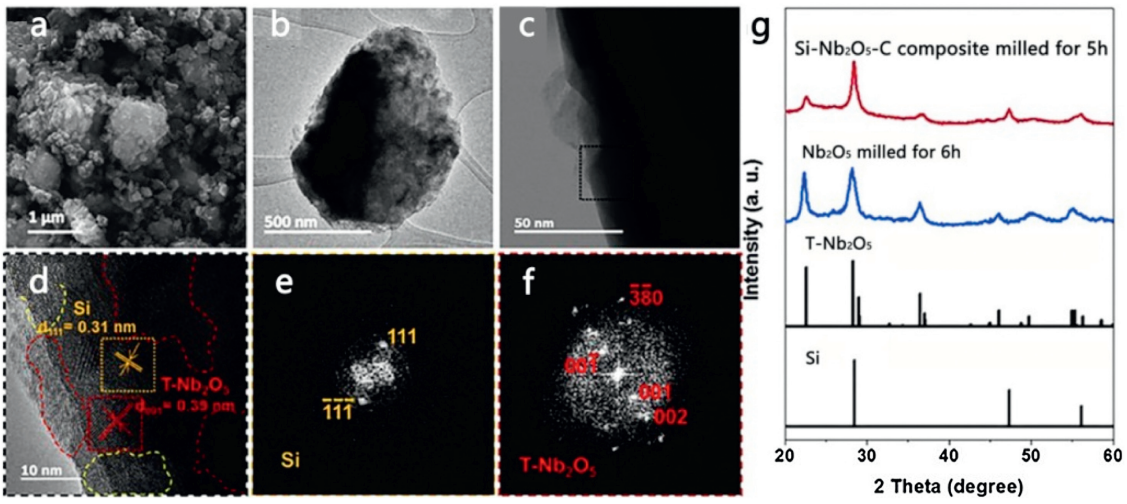

Fig. 7. (a–f) Electron microscope analyzes about Si-SiO_x-Nb_2O_5-C composites: (a) FE-SEM graphics, (b) low-magnification TEM graphics, (c) high-magnification TEM graphics, (d) HR-TEM graphics, and (e, f) FFT graph for chose areas in the HR-TEM graphics. (g) XRD graph of 6 h-milled Nb_2O_5 and 5 h-milled Si-Nb_2O_5-C composites. Reproduced with permission [127]. Copyright 2017, Elsevier.

to the unique characteristics of the Si@SiO_x/Ni/graphite composites: (1) Si@SiO_x/Ni/graphite had a specific compositional structure; (2) nano-Si/oxide had a rich electrochemical activity; and (3) the nano-Ni/graphite coating and crosslinked matrix served as an electrical highway and a mechanical skeleton. Therefore, the composite exhibited excellent electrochemical performance, such as a great reversible capacity, a high CE and good cycling performance.

5. Influence factors

The structure and properties of SiO_x ($0 < x \leq 2$), the structure of the resulting SiO_x-based composites, and the electrolytes, additives, binders and doped layers all influence the electrochemical properties of the SiO_x-based composites.

SiO_x ($0 < x \leq 2$) is an amorphous material with an internal structure that is difficult to characterize by conventional means. There are two main structural models of SiO_x in the early stage: one is a "random bond" model (RB model), and the other is a "random mix" model (RM model). Based on diffraction, microscopy, spectroscopy, and magnetometry results, Hohl *et al.* [130] put forward an interface cluster model (ICM), which proposed shapeless SiO as a frozen nonequilibrium setup of disproportionation in the starting stage. Because of the limited dimensional resolution of these measurements, such as TEM, XRD, and XPS, average or spectral information about amorphous SiO structures was provided. Hirata *et al.* [131] observed the atomic-scale resolution of SiO_x by high-energy XRD, Angstrom-beam electron diffraction, and computational simulations to further prove the interface cluster model (ICM). The electrochemical performance of the SiO_x materials is closely related to the oxygen content *x*. Early reports [132–134] showed that the specific capacity of SiO_x decreased gradually following an increase of *x*, while its cyclic performance increased slightly.

SiO_x-based composites generally have improved electrochemical properties over those of SiO_x, but the materials that combine with SiO_x have their own advantages in terms of electrochemical performance (*e.g.*, reversible capacity, magnification, and thermal stability). Improvements in electrochemical performance are not only related to the composite material but also to the morphology of the SiO_x-based composite. The porous structure is the most common topography of SiO_2 composites, SiO composites and SiO_x ($0 < x < 2$) composites. In addition, the common morphology of SiO composites also has NPs. The morphological structure of SiO_2 composites and SiO_x ($0 < x < 2$) composites also have layered structure, spherical structure, shell-core structure, *etc.* However, some SiO_x-based composites fabricated with the same material but different nanostructures (*e.g.*, reticular nanostructures, shell-core nanostructures, and nanotube structures) also exhibit somewhat different electrochemical properties. Porous structure is the most common topographical structures of SiO_x-based composites.

The SiO_x composite electrode experiences solid electrolyte interphase (SEI) layer growth [135] *via* the reductive decomposition of the electrolyte solution in the process of charging, and continuously formed cracks after the first charging-discharging cycle cause continuous growth of the SEI film, thereby exposing a new surface to the electrolyte. This reduces the electrochemical performance of the SiO_x composite electrode to a certain extent. The SEI is a passivation layer formed by reacting an electrode material with an electrolyte at a solid-liquid phase interface in a first cycle. The presence of SEI can inhibit further decomposition of the electrolyte and increase the cycle life of the LIB. However, it generates irreversible capacity when consuming Li^+, and hinders deintercalation of Li^+. Electrolyte solutions are a key factor affecting the formation of SEI. The electrolyte solution is mainly prepared by a certain ratio of an organic solvent, an electrolyte lithium salt and an additive under certain conditions. $LiPF_6$ is the most common electrolyte. Commonly used organic solvent systems are: EC + DMC, EC + DEC, EC + DMC + EMC and EC + DMC + DEC, *etc.* The use of additives can further improve the electrolyte solution, such as fluoroethylene carbonate (FEC) [136], vinylene carbonate (VC) [113] and silicone (siloxane) [137]. These studies also found that additives can improve the electrochemical performance of SiO_x composites to some extent. In addition to being used as a negative electrode material for LIBs, SiO_2-based materials are also often used as their electrolyte materials. Vélez *et al.* [138] synthesized organic – inorganic hybrid solid electrolytes that based on silica – polyethylene glycol PEG (200, 400) with bis-(trifluoromethane) sulfonimide lithium salt or lithium trifluoromethanesulfonate *via* sol – gel method. Hu and Choudhury *et al.* [139,140] also prepared solid electrolytes related to SiO_2.

The binder has an important effect on the cycle performance of high specific volume SiO_x-based anode materials that exhibit volume expansion. Due to the poor performance of the traditional binder polyvinylidene fluoride (PVDF), some studies have proposed new binders such as polyimide (PI) [141,142], sodium carboxymethyl cellulose (CMC) [143,144], polyacrylic acid (PAA) [145,146], polyvinyl alcohol (PVA) [146] and sodium alginate (Alg) [147]. These new binders allow for better cycling of SiO_x-based electrodes for the following reasons: (1) weak interplays between the adhesive and the electrolyte; (2) they offer a Li^+ path to the surface of SiO_x; and (3) they help create a transformable and steady SEI layer on the SiO_x surface. To prove that different binders have different effects on the electrochemical properties of SiO_x composites, Guerfi *et al.* [148] studied the electrochemical performance of three types of adhesives (PVDF, CMC-based water dispersion (WDB) and polyamide) on SiO_x/C or SiO_x/C-graphite composites. The study found that the order of increasing CE for the electrodes based on these binders was as follows: WDB, polyamide and PVDF. Later, Komaba *et al.* [145] studied the effects of PAA, CMCNa and PVDF binders on the SiO_x cycle and found that the PAA adhesive exhibited the best performance. Thus, the electrochemical performances of the binder and the SiO_x composite electrode are closely related.

Doped layers also have an influence on the electrochemical properties of the SiO_x composite electrodes. A doped carbon coating is the most commonly used approach. Carbon coatings can provide high conductivity, surface protection, and tough substrates that accommodate volume changes in SiO_x electrodes. To improve the rapid charging and discharging performance of the SiO_x/C composite electrode, nitrogen was introduced into the carbon coating. The addition of nitrogen [86,149] increased the spacing between the graphite layers, which boosted Li^+ transport and increased the electronic conductivity of carbon. Boron doping was also found to improve the electrochemical performance of SiO_x composite electrodes.

6. Conclusions and outlooks

In summary, SiO_x-based ($0 < x \leq 2$) composites are promising LIB high specific capacity anode material. Although SiO_x has a higher specific capacity and a smaller volume change than Si, SiO_x also suffers from a low ICE and poor cycling stability. Compounding with a second phase (such as C, Si and MO_x) is one of the commonly used methods to improve the electrochemical properties of SiO_x. As far as the composite itself, the electrochemical properties of SiO_x-based composites are closely related to the properties, content and structure of the materials that compound with SiO_x. Different composite materials exhibit different electrochemical performance: SiO_x/C composites have a high electrical conductivity and a smaller volume expansion, thus demonstrating a better cycling stability and rate performance, while SiO_x/Si composites

and SiO_x/MO_x composites both have a high ICE and capacity retention. In addition, modulating the ratio of reactants, the synthesized product generally exhibits different electrochemical properties. Desirable carbon content in the SiO_x/C composites is beneficial for improving the electrochemical performances of SiO_x and excessive carbon will reduce the overall capacity of the composites. The nanostructures of the materials that compound with SiO_x also play a critical impact on its electrochemical properties. For example, in Si/SiO_x composites, the nanostructure of Si has different effects on the electrochemical properties of Si/SiO_x composites. When Si is NPs [150], it provides a more stable recycling of Si and avoids contact with the flexible substrate. However, the volume expansion and pulverization of the Si NPs can reduce the capacity. When Si is nanowires [151], in the process of lithiation/delithiation, its unique structure offers extra expansion airspace and avoids the crushing of Si. In addition, for nanostructures with high aspect ratios, the lithium diffusion range is greatly reduced, allowing rapid ion transfer and rate dynamics. For the above reasons, studies have shown that porous nanomaterial and $MO_x/C/SiO_x(0 < x \leq 2)$ materials exhibit more outstanding electrochemical properties than general nanostructures and general composite materials. It can be seen that SiO_x-based $(0 < x \leq 2)$ composites will develop into porous multiphase composites.

In general, the electrochemical performance of SiO_x composite materials are improved compared to that of pure SiO_x. However, there are still some problems to be addressed in the development of SiO_x-based composites: (1) The ICE of SiO_x-based composites is still not high enough, which in practice will consume a large amount of Li^+ from the cathode material, resulting in a reduction in battery energy density; (2) The nanostructures of the SiO_x-based composites are imperfect, requiring new thinking about the lithiation/delithiation mechanism of the oxide surface; (3) The factors affecting the electrochemical performance of SiO_x-based composites still need further study; (4) For practical LIB applications, the preparation method and the fine process of SiO_x-based composites have yet to be further explored. It is believed that, in the near future, SiO_x-based composites will be applied on a large scale.

Acknowledgments

This work was supported by the National Natural Science Foundation of China (NSFC, Nos. 21671170, 21673203 and 21201010), the Top-notch Academic Programs Project of Jiangsu Higher Education Institutions (TAPP), Program for New Century Excellent Talents of the University in China (NCET, No. 13-0645) and Postgraduate Research & Practice Innovation Program of Jiangsu Province (No. XSJCX17-015). We also acknowledge the Priority Academic Program Development of Jiangsu Higher Education Institutions and the technical support we received at the Testing Center of Yangzhou University.

References

[1] K. Huang, B. Li, M. Zhao, et al., Chin. Chem. Lett. 28 (2017) 2195–2206.
[2] F. Wang, Y. Liu, Y.F. Zhao, et al., Appl. Sci.-Basel 8 (2018) 22–28.
[3] J.L. Ma, F.Z. Ren, G.X. Wang, et al., Int. J. Hydrogen Energy 42 (2017) 11654–11661.
[4] R. Marom, S.F. Amalraj, N. Leifer, D. Jacob, D. Aurbach, J. Mater. Chem. 21 (2011) 9938–9954.
[5] M.M. Thackeray, C. Wolverton, E.D. Isaacs, Synth. Lect. Energy Environ. Technol. Sci. Soc. 5 (2012) 7854–7863.
[6] D. Shi, R. Zheng, M.J. Sun, et al., Angew. Chem. Int. Ed. 56 (2017) 14637–14641.
[7] Y. Li, J. Song, J. Yang, Renew. Sust. Energy. Rev. 37 (2014) 627–633.
[8] C.S. Liu, C.X. Sun, J.Y. Tian, et al., Biosens. Bioelectron. 91 (2017) 804–810.
[9] C.S. Liu, Z.H. Zhang, M. Chen, et al., Chem. Commun. (Camb.) 53 (2017) 3941–3944.
[10] H. Yuan, L. Kong, T. Li, Q. Zhang, Chin. Chem. Lett. 28 (2017) 2180–2194.
[11] C. Yang, X. Zhong, Y. Jiang, Y. Yu, Chin. Chem. Lett. 28 (2017) 2231–2234.
[12] P. Meduri, J.H. Kim, H.B. Russell, et al., J. Phys. Chem. C 114 (2010) 10621–10627.
[13] D.M. Chen, J.Y. Tian, Z.W. Wang, et al., Chem. Commun. (Camb.) 53 (2017) 10668–10671.
[14] S. Zhang, X. Ge, C. Chen, Chin. Chem. Lett. 28 (2017) 2274–2276.
[15] A.K. Shukla, T.P. Kumar, Curr. Sci. 94 (2008) 314–331.
[16] M. Zhou, Y. Liu, J. Chen, X. Yang, J. Mater. Chem. A Mater. Energy Sustain. 3 (2015) 1068–1076.
[17] B. Zhao, S.Y. Huang, T. Wang, et al., J. Power Sources 298 (2015) 83–91.
[18] Y. Xia, G. Wang, X. Zhang, B. Wang, H. Wang, Electrochim. Acta 220 (2016) 643–653.
[19] X. Ao, J. Jiang, Y. Ruan, et al., J. Power Sources 359 (2017) 340–348.
[20] S.J. Kim, S.H. Moon, M.C. Kim, et al., J. Appl. Electrochem. 48 (2018) 1057–1068.
[21] W. Tang, X. Guo, X. Liu, et al., Appl. Clay Sci. 162 (2018) 499–506.
[22] X. Zhou, S. Chen, H. Zhou, et al., Microporous Mesoporous Mater. 268 (2018) 9–15.
[23] M.S. Wang, Z.Q. Wang, R. Jia, et al., Appl Surface Sci. 456 (2018) 379–389.
[24] M. Dirican, Y. Lu, K. Fu, H. Kizil, X. Zhang, RSC Adv. 5 (2015) 34744–34751.
[25] C. Huang, A. Kim, D.J. Chung, et al., ACS Appl. Mater. Interfaces 10 (2018) 15624–15633.
[26] J.I. Lee, N.S. Choi, S. Park, Energy Environ. Sci. 5 (2012) 7878–7882.
[27] U. Kasavajjula, C. Wang, A.J. Appleby, J. Power Sources 163 (2007) 1003–1039.
[28] L. Wei, Z. Hou, H. Wei, Electrochim. Acta 229 (2017) 445–451.
[29] Y. Ma, H. Tang, Y. Zhang, et al., J. Alloys. Compd. 704 (2017) 599–606.
[30] H. Jung, B.C. Yeo, K.R. Lee, S.S. Han, Phys. Chem. Chem. Phys. 18 (2016) 32078–32086.
[31] R. Miyazaki, N. Ohta, T. Ohnishi, K. Takada, J. Power Sources 329 (2016) 41–49.
[32] C. Liang, L. Zhou, C. Zhou, et al., Mater. Res. Bull. 96 (2017) 347–353.
[33] X. Luo, H. Zhang, W. Pan, et al., Small 11 (2015) 6009–6012.
[34] J. Zhang, J. Zhang, D. Wang, X. Xie, B. Xia, Mater. Lett. 190 (2017) 79–82.
[35] H. Takezawa, S. Ito, H. Yoshizawa, T. Abe, Chem. Lett. 46 (2017) 1365–1367.
[36] H. Takezawa, S. Ito, H. Yoshizawa, T. Abe, J. Power Sources 324 (2016) 45–51.
[37] J.H. Kim, H.J. Sohn, H. Kim, G. Jeong, W. Choi, J. Power Sources 170 (2007) 456–459.
[38] J. Zhang, J. Gu, H. He, M. Li, J. Solid State Electrochem. 21 (2017) 2259–2267.
[39] B. Kurc, Ionics 24 (2018) 121–131.
[40] F. Dai, R. Yi, M.L. Gordin, S. Chen, D. Wang, RSC Adv. 2 (2012) 12710–12713.
[41] J. Cui, F. Cheng, J. Lin, et al., Powder Technol. 311 (2017) 1–8.
[42] J. Woo, S.H. Baek, J.S. Park, Y.M. Jeong, J.H. Kim, J. Power Sources 299 (2015) 25–31.
[43] J. Bae, D.S. Kim, H. Yoo, et al., ACS Appl. Mater. Interfaces 8 (2016) 4541–4547.
[44] X. Zhu, D. Yang, J. Li, F. Su, J. Nanosci. Nanotechnol. 15 (2015) 15–30.
[45] F. Luo, B. Liu, J. Zheng, et al., J. Electrochem. Soc. 162 (2015) A2509–A2528.
[46] J.Y. Li, Q. Xu, G. Li, et al., Mater. Chem. Front. 1 (2017) 1691–1708.
[47] T. Chen, J. Wu, Q. Zhang, X. Su, J. Power Sources 363 (2017) 126–144.
[48] M.T. McDowell, S.W. Lee, W.D. Nix, Y. Cui, Adv. Mater. 25 (2013) 4966–4984.
[49] M. Winter, G.H. Wrodnigg, J.O. Besenhard, W. Biberacher, P. Novák, J. Electrochem. Soc. 147 (2000) 2427–2431.
[50] H.H. Li, L.L. Zhang, C.Y. Fan, et al., Phys. Chem. Chem. Phys. 17 (2015) 22893–22899.
[51] H. Xia, Z. Yin, F. Zheng, Y. Zhang, Mater. Lett. 205 (2017) 83–86.
[52] Y. Hou, H. Yuan, H. Chen, J. Shen, L. Li, Ceram. Int. 43 (2017) 11505–11510.
[53] Z. Qiang, X. Liu, F. Zou, et al., J. Phys. Chem. C 121 (2017) 16702–16709.
[54] L. Zhang, K. Shen, W. He, Y. Liu, S. Guo, J. Electrochem. Sci. 12 (2017) 10221–10229.
[55] Y. Hyun, J.Y. Choi, H.K. Park, J.Y. Bae, C.S. Lee, Mater. Res. Bull. 82 (2016) 92–101.
[56] Y. Liang, L. Cai, L. Chen, et al., Nanoscale 7 (2015) 3971–3975.
[57] H. Wang, P. Wu, M. Qu, et al., ChemElectroChem 2 (2015) 508–511.
[58] L. Yin, M. Wu, Y. Li, et al., New Carbon Mater. 32 (2017) 311–318.
[59] S. Hao, Z. Wang, L. Chen, Mater. Des. 111 (2016) 616–621.
[60] T.T. Zuo, Y.X. Yin, S.H. Wang, P.F. Wang, Nano Lett. 18 (2018) 297–301.
[61] D. Jia, K. Wang, J. Huang, Chem. Eng. J. 317 (2017) 673–686.
[62] X. Cao, X. Chuan, R.C. Massé, et al., J. Mater. Chem. A Mater. Energy Sustain. 3 (2015) 22739–22749.
[63] W. Xiao, C. Miao, X. Yan, P. Mei, Ionics 21 (2015) 2149–2153.
[64] Y. Zhou, Z. Tian, R. Fan, et al., Powder Technol. 284 (2015) 365–370.
[65] R. Fu, K. Zhang, R.P. Zaccaria, et al., Nano Energy 39 (2017) 546–553.
[66] D. Shen, C. Huang, L. Gan, et al., ACS Appl. Mater. Interfaces 10 (2018) 7946–7954.
[67] Y. Hu, X. Liu, X. Zhang, et al., Electrochim. Acta 190 (2016) 33–39.
[68] J. Su, J. Zhao, L. Li, et al., ACS Appl. Mater. Interfaces 9 (2017) 17807–17813.
[69] K. Xiao, Q. Tang, Z. Liu, et al., Ceram. Int. 44 (2017) 3548–3555.
[70] T. Yang, X. Tian, X. Li, et al., Chem. -Eur. J. 23 (2017) 2165–2170.
[71] J. Wang, X. Hou, M. Zhang, et al., Silicon 9 (2017) 97–104.
[72] Y. Wang, W. Zhou, L. Zhang, G. Song, S. Cheng, RSC Adv. 5 (2015) 63012–63016.
[73] D.W. Choi, K.L. Choy, Dalton Trans. 46 (2017) 14226–14233.
[74] G. Lee, S. Kim, S. Kim, J. Choi, Adv. Funct. Mater. 27 (2017) 1703538.
[75] D.W. Choi, K.L. Choy, Electrochim. Acta 218 (2016) 47–53.
[76] A. Tarafdar, A.B. Panda, P. Pramanik, Microporous Mesoporous Mater. 84 (2005) 223–228.
[77] K. Siwińska-Stefańska, B. Kurc, J. Electrochem. Soc. 164 (2017) A728–A734.
[78] E.Y. Evschik, D.V. Novikov, V.I. Berestenko, et al., Russ. Chem. Bull. 65 (2016) 1986–1989.

[79] D.V. Novikov, E.Y. Evschik, V.I. Berestenko, et al., Electrochim. Acta 208 (2016) 109–119.
[80] C. Tang, N. Li, J. Sheng, et al., J. Electrochem. Soc. 164 (2017) A6110–A6115.
[81] S. Han, Y. Zhao, Y. Tang, et al., Carbon. 81 (2015) 203–209.
[82] J.Y. Kim, D.T. Nguyen, J.S. Kang, S.W. Song, J. Alloys. Compd. 633 (2015) 92–96.
[83] X. Yuan, H. Xin, X. Qin, et al., Electrochim. Acta 155 (2015) 251–256.
[84] L. Shi, C. Pang, S. Chen, et al., Nano Lett. 17 (2017) 3681–3687.
[85] Y. Li, X. Hou, J. Wang, et al., J. Mater. Sci. Mater. Electron. 26 (2015) 7507–7514.
[86] D.J. Lee, M.H. Ryou, J.N. Lee, et al., Electrochem. Commun. 34 (2013) 98–101.
[87] X. Huang, M. Li, Appl. Surf. Sci. 439 (2018) 336–342.
[88] H. Morimoto, D. Higuchi, S. Tobishima, Electrochemistry 83 (2015) 813–816.
[89] J.H. Yom, J.K. Lee, W.Y. Yoon, J. Appl. Electrochem. 45 (2015) 397–403.
[90] F. Dou, L. Shi, P. Song, et al., Chem. Eng. J. 338 (2018) 488–495.
[91] F. Cheng, G. Wang, Z. Sun, et al., Ceram. Int. 43 (2017) 4309–4313.
[92] G. Jeong, J.H. Kim, Y.U. Kim, Y.J. Kim, J. Mater. Chem. 22 (2012) 7999–8004.
[93] A. Yamano, M. Morishita, M. Yanagida, T. Sakai, J. Electrochem. Soc. 162 (2015) A1730–A1737.
[94] M. Li, Y. Yu, J. Li, et al., J. Power Sources 293 (2015) 976–982.
[95] Z. Sun, X. Wang, T. Cai, Z. Meng, W.Q. Han, RSC Adv. 6 (2016) 40799–40805.
[96] Y. Ren, X. Wu, M. Li, Electrochim. Acta 206 (2016) 328–336.
[97] Q. Xu, J.K. Sun, G. Li, et al., Chem. Commun. (Camb.) 53 (2017) 12080–12083.
[98] P. Lv, H. Zhao, C. Gao, et al., J. Power Sources 274 (2015) 542–550.
[99] Q. Xu, J.K. Sun, Y.X. Yin, Y.G. Guo, Adv. Funct. Mater. 28 (2017) 1705235.
[100] W. Wu, J. Shi, Y. Liang, et al., Phys. Chem. Chem. Phys. 17 (2015) 13451–13456.
[101] J.H. Cheon, B.Y. Jang, J.S. Kim, J.S. Lee, C.H. Cho, J. Korean Phys. Soc. 62 (2013) 1119–1124.
[102] L. Shi, W. Wang, A. Wang, et al., J. Power Sources 318 (2016) 184–191.
[103] C. Gao, H. Zhao, P. Lv, et al., J. Electrochem. Soc. 161 (2014) A2216–A2221.
[104] J. Zhang, X. Zhang, C. Zhang, et al., Energy Fuels 31 (2017) 8758–8763.
[105] J. Zhang, C. Zhang, Z. Liu, et al., J. Power Sources 339 (2017) 86–92.
[106] Z. Li, Q. He, L. He, et al., J. Mater. Chem. A: Mater. Energy Sustain. 5 (2017) 4183–4189.
[107] J. Cui, Y. Cui, S. Li, et al., ACS Appl. Mater. Interfaces 8 (2016) 30239–30247.
[108] Y. Chen, L. Liu, J. Xiong, et al., Adv. Funct. Mater. 25 (2015) 6701–6709.
[109] Y. Chen, Y. Lin, N. Du, et al., Chem. Commun. (Camb.) 53 (2017) 6101–6104.
[110] J. Lee, J. Koo, B. Jang, S. Kim, J. Power Sources 329 (2016) 79–87.
[111] E. Park, J. Kim, D.J. Chung, et al., ChemSusChem 9 (2016) 2754–2758.
[112] F. Somodi, C.S. Kong, J.C. Santos, D.E. Morse, New J. Chem. 39 (2015) 621–630.
[113] Y.S. Hu, R. Demir-Cakan, M.M. Titirici, et al., Angew. Chem. Int. Ed. 47 (2008) 1645–1649.
[114] J. Niu, S. Zhang, Y. Niu, et al., J. Mater. Chem. A: Mater. Energy Sustain. 3 (2015) 19892–19900.
[115] B. Jiang, S. Zeng, H. Wang, et al., ACS Appl. Mater. Interfaces 8 (2016) 31611–31616.
[116] Y. Sun, L. Fan, W. Li, et al., RSC Adv. 6 (2016) 101008.
[117] M. Zhu, J. Yang, Z. Yu, H. Chen, F. Pan, J. Mater. Chem. A: Mater. Energy Sustain. 5 (2017) 7026–7034.
[118] S.J. Lee, H.J. Kim, T.H. Hwang, et al., Nano Lett. 17 (2017) 1870–1876.
[119] Y. Li, Z. Long, P. Xu, et al., Inorg. Chem. Front. 4 (2017) 1996–2004.
[120] J. Gu, Y. Zeng, X. Feng, X. Wu, C. Zeng, M. Li, J. Alloys. Compd. 662 (2016) 185–192.
[121] X. Bai, Y. Yu, H.H. Kung, B. Wang, J. Jiang, J. Power Sources 306 (2016) 42–48.
[122] L. Qian, J.L. Lan, M. Xue, Y. Yu, X. Yang, RSC Adv. 7 (2017) 36697–36704.
[123] X. Zhuang, P. Song, G. Chen, et al., ACS Appl. Mater. Interfaces 9 (2017) 28464–28472.
[124] C. Hoeltgen, J.E. Lee, B.Y. Jang, Electrochim. Acta 222 (2016) 535.
[125] H. He, D. Kong, B. Wang, et al., Adv. Energy Mater. 6 (2016) 1502495.
[126] K. Kim, M.S. Kim, H. Choi, et al., Electron. Mater. Lett. 13 (2017) 152–159.
[127] M.S. Kim, K. Kim, P.R. Cha, et al., J. Alloys. Compd. 699 (2017) 351–357.
[128] T. Tashiro, M. Kaga, M. Kambara, J. Appl. Phys. 54 (2015) 01AD03.
[129] J. Wang, W. Bao, L. Ma, et al., ChemSusChem 8 (2015) 4073–4080.
[130] A. Hohl, T. Wieder, P.A. Van. Aken, et al., J. Non. Solids 320 (2003) 255–280.
[131] A. Hirata, S. Kohara, T. Asada, et al., Nat. Commun. 7 (2016) 1–7.
[132] J. Yang, Y. Takeda, N. Imanishi, et al., Solid State Ion. 152 (2002) 125–129.
[133] H. Takezawa, K. Iwamoto, S. Ito, H. Yoshizawa, J. Power Sources 244 (2013) 149–157.
[134] Y. Ren, M. Li, J. Power Sources 306 (2016) 459–466.
[135] Q. Si, K. Hanai, T. Ichikawa, et al., J. Power Sources 196 (2011) 9774–9779.
[136] N.S. Choi, K.H. Yew, K.Y. Lee, et al., J. Power Sources 161 (2006) 1254–1259.
[137] C.C. Nguyen, H. Choi, S.W. Song, J. Electrochem. Soc. 160 (2013) A906–A914.
[138] J.F. Ve'lez, M. Aparicio, J. Mosa, J. Phys. Chem. C 120 (2016) 22852–22864.
[139] J. Hu, W. Wang, H. Peng, et al., Macromolecules 50 (2017) 1970–1980.
[140] S. Choudhury, S. Stalin, Y. Deng, L.A. Archer, Chem. Mater. 30 (2018) 5996–6004.
[141] T. Miyuki, Y. Okuyama, T. Sakamoto, et al., Electrochemistry 80 (2012) 401–404.
[142] R. Yuge, A. Toda, K. Fukatsu, et al., J. Electrochem. Soc. 160 (2013) A1789–A1793.
[143] J.H. Yom, S.W. Hwang, S.M. Cho, W.Y. Yoon, J. Power Sources 311 (2016) 159–166.
[144] X. Feng, J. Yang, X. Yu, J. Wang, Y. Nuli, J. Solid State Electrochem. 17 (2013) 2461–2469.
[145] S. Komaba, K. Shimomura, N. Yabuuchi, et al., J. Phys. Chem. C 115 (2019) 13487–13495.
[146] A. Magasinski, B. Zdyrko, I. Kovalenko, et al., ACS Appl. Mater. Interfaces 2 (2010) 3004–3010.
[147] I. Kovalenko, B. Zdyrko, A. Magasinski, et al., Science 334 (2011) 75–79.
[148] A. Guerfi, P. Charest, M. Dontigny, et al., J. Power Sources 196 (2011) 5667–5673.
[149] W.H. Shin, H.M. Jeong, B.G. Kim, J.K. Kang, J.W. Choi, Nano Lett. 12 (2012) 2283–2288.
[150] T. Zhang, J. Gao, H.P. Zhang, et al., Electrochem. Commun. 9 (2007) 886–890.
[151] E. Park, M.S. Park, J. Lee, et al., ChemSusChem 8 (2015) 688–694.

Biography of corresponding author

Huan Pang received his PhD degree from Nanjing University in 2011. He now is a university distinguished professor in Yangzhou University and the managing editor of EnergyChem, Elsevier. In the past 10 years, his group has been engaged in the design and synthesis of functional nanomaterials, especially for MOF-based materials. He has published more than 200 papers in peer-reviewing journals including *Chem. Soc. Rev.*, *Adv. Mater.*, *Energy Environ. Sci.*, with 7400 citations (H-index = 52). His research interests include the development of inorganic nanostructures and their applications in nanoelectrochemistry with a focus on energy devices.